SURVEY AND LOGISTICS REPORT ON A HELICOPTER BORNE VERSATILE TIME DOMAIN ELECTROMAGNETIC (VTEM) SURVEY

on the

BUNDARRA PROJECT AREA

AUSTRALIA

for

REGENCY MINES AUSTRALASIA PTY LIMITED

by

GEOTECH AIRBORNE PTY LIMITED

Unit 1, 29 Mulgul Road,
Malaga, WA, 6090,
Australia
Tel: +61-8-9249-8814
Fax: +61-8-9249-8894
www.geotechairborne.com
e-mail: info@geotechairborne.com

Project AA1053
September, 2011

TABLE OF CONTENTS

APPENDICES

SURVEY AND LOGISTICS REPORT ON A HELICOPTER-BORNE VTEM SURVEY

1. SURVEY SPECIFICATIONS

1.1. General

Job Number	AA1053
Client	Regency Mines Australasia Pty Ltd.
Project Area	Bundarra
Location	Australia
Number of Blocks	5
Total line kilometres	1111.6
Survey date	23 September to 4 October
Client Representative	Helen Salmon Tel: +44 207 402 4580 helen.salmon@regency-mines.com
Client address	Unit A14 - 550 Canning Hwy Attadale, 6156, Western Australia

1.2. VTEM flight plan on Google EARTH^{TM} Background

Regency Mines Australasia Pty Ltd
Bundarra, Australia
VTEM Flight Plans
Google Earth™ Background
Geotech Airborne Pty Limited

23 September 2011

1.3. Survey block coordinates.

Easting UTM Z 55S	Northing UTM Z 55S
AREA 1	
654773	7575828
661970	7575828
661993	7573927
663678	7573919
663678	7570920
660431	7570920
660439	7572992
656203	7572992
654773	7574970
654780	7575836
AREA 2	
654781	7575066
651763	7566425
653704	7565780
656241	7573044
AREA 3	
663613	7565227
664145	7565947
666982	7565947
666982	7567396
659200	7567388
657700	7568721
654728	7568720
653704	7565780
655341	7565217
663613	7565227
AREA 4	
661072	7568364
664072	7568364
664072	7569864
661072	7569864
661072	7568364
AREA 5	
651744	7574848
648778	7566443
652216	7563567
650216	7563522
650710	7562892
651946	7562555
656464	7562510

656688	7562825
658801	7562847
658756	7563656
660823	7563656
660891	7564398
663835	7564398
663745	7565274
655340	7565252
651812	7566466
654845	7574893
651722	7574871

1.4. Survey block specifications

Survey block	Line spacing (m)	Line-km (contractual)	Line-km (delivered)	Flight direction	Line number
BLOCK 1	100	266	269.9	090°- 270°	L10010-L10490
BLOCK 2	100	177	178.3	019°- 199°	L20010-L20210
BLOCK 3	100	310	313.2	090°- 270°	L30010-L30350
BLOCK 4	100	45	46.2	090°- 270°	L40010-L40150
BLOCK 5	200	295	304.0	090°- 270°	L49965-L50610

1.5. Survey schedule

Date	Flight #	Block	Nominal Production Km flown	Comments
23-Sep-11				Waiting for crew
24-Sep-11				No production
25-Sep-11				No production
26-Sep-11	1,2,3			VTEM assembly and tests
27-Sep-11	4,5,6,7,8			VTEM assembly and tests
28-Sep-11	9			VTEM assembly and tests
29-Sep-11	10,11,12	5	120.2	F12 Production. F10 test. F11 ferry
30-Sep-11	13,14,15	1,2,5	480.4	Production.
01-Oct-11				No production. High winds
02-Oct-11	16	1	69.2	Production. High winds
03-Oct-11	17,18,19	2,3,4	382.6	Production
04-Oct-11	20,21	3	39.9	Production

2. SYSTEM SPECIFICATIONS

2.1. Instrumentation

Survey Helicopter	
Model	SA 315 B3
Registration	VH-VTN
Operating Company	United Aero Helicopters
Nominal survey speed	80 km/h
Nominal terrain clearance	80 m
VTEM Transmitter	
Coil diameter	26 m
Number of turns	4
Pulse repetition rate	25 Hz
Peak current	200 Amp
Duty cycle	41.7%
Peak dipole moment	425,000
Pulse width	8.36 ms
Nominal terrain clearance	48 m
VTEM Receiver	
Coil diameter	1.2 metre
Number of turns	100
Effective area	113.1 m^2
Sampling interval	0.1 s
Nominal terrain clearance	48 m
Magnetometer	
Type	Geometrics
Model	Optically pumped cesium vapour
Sensitivity	0.02 nT
Sampling interval	0.1 s
Cable length	13.115 m
Nominal terrain clearance	70 m
Radar Altimeter	
Type	Terra TRA 3000/TRI 40
Position	Beneath cockpit
Sampling interval	0.2 s
GPS navigation system	
Type	NovAtel
Model	WAAS enabled OEM4-G2-3151W
Antenna position	Helicopter tail
Sampling interval	0.2 s
Base Station Magnetometer/GPS	
Type	Geometrics
Model	Cesium vapour
Sensitivity	0.001 nT
Sampling interval	1 s

2.2. VTEM Configuration

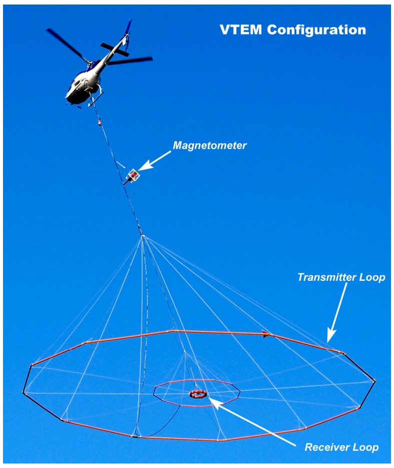

Configuration	
Cable angle with vertical	40 °
Cable length (EM receiver)	41.5 m
Cable length (Magnetometer)	13. m

2.3. VTEM decay sampling scheme

VTEM B-field System Decay Sampling scheme				
Array Index	Microseconds			
	Middle	Start	End	Width
13	83	78	90	12
14	96	90	103	13
15	110	103	118	15
16	126	118	136	18
17	145	136	156	20
18	167	156	179	23
19	192	179	206	27
20	220	206	236	30
21	253	236	271	35
22	290	271	312	40
23	333	312	358	46
24	383	358	411	53
25	440	411	472	61
26	505	472	543	70
27	580	543	623	81
28	667	623	716	93
29	766	716	823	107
30	880	823	945	122
31	1010	945	1086	141
32	1161	1086	1247	161
33	1333	1247	1432	185
34	1531	1432	1646	214
35	1760	1646	1891	245
36	2021	1891	2172	281
37	2323	2172	2495	323
38	2667	2495	2865	370
39	3063	2865	3292	427
40	3521	3292	3781	490
41	4042	3781	4341	560
42	4641	4341	4987	646
43	5333	4987	5729	742
44	6125	5729	6581	852
45	7036	6581	7560	979
46	8083	7560	8685	1125
47	9286	8685	9977	1292

2.4. VTEM Transmitter Waveform over one half-period (September 2011)

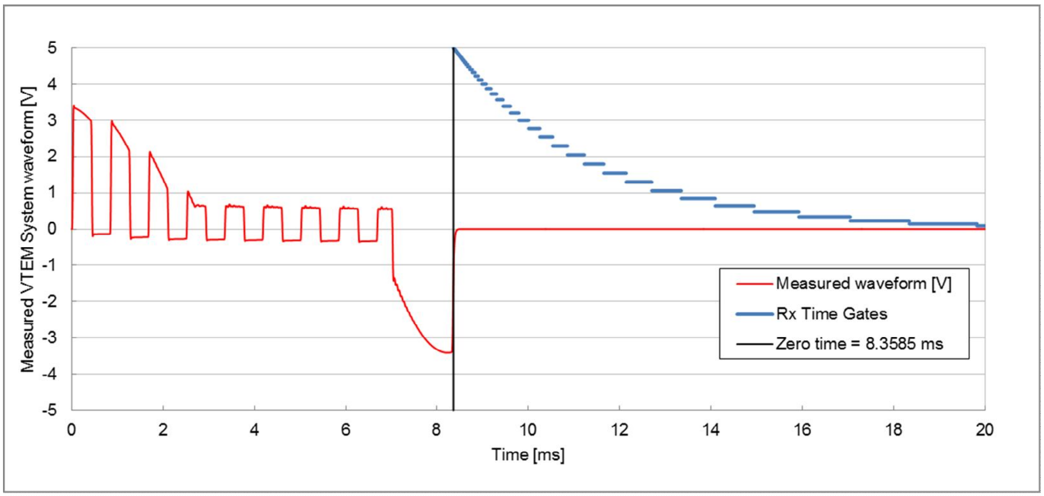

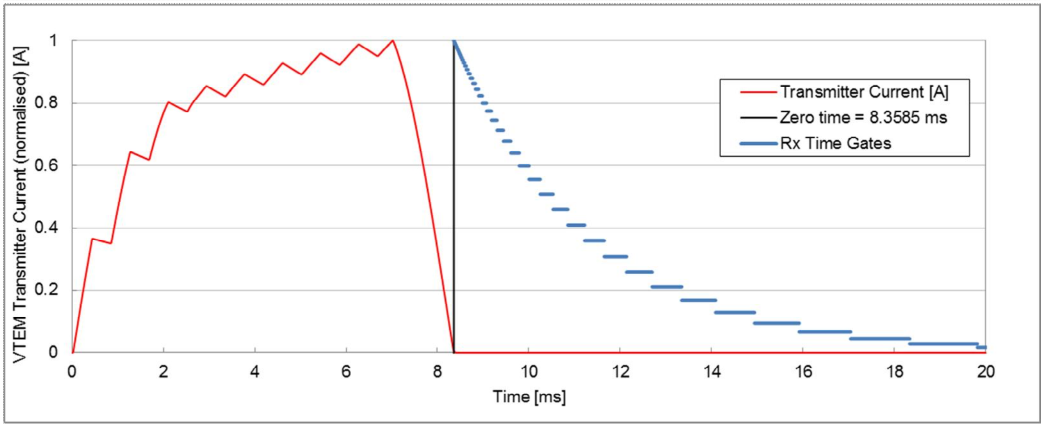

3. PROCESSING

3.1. Processing parameters

Coordinates	
Projection	MGA Z55
Datum	GDA94
Spheroid	GDA94
Spherics rejection (EM and Magnetic data)	
Non-linear filter	4 point
Non-linear filter sensitivity	0.0001
Low-pass filter wavelength	15 fids
Lag correction of other sensors to EM receiver position	
GPS	19 m
Radar	30 m
Magnetometer	18 m

3.2. Flight Path

The flight path, recorded by the acquisition program as WGS 84 latitude/longitude, was converted into the UTM coordinate system in Oasis Montaj. The flight path was drawn using linear interpolation between x,y positions from the navigation system. Positions are updated every second and expressed as UTM eastings (x) and UTM northings (y).

3.3. Electromagnetic Data

A three stage digital filtering process was used to reject major sferic events and to reduce system noise. Local sferic activity can produce sharp, large amplitude events that cannot be removed by conventional filtering procedures. Smoothing or stacking will reduce their amplitude but leave a broader residual response that can be confused with geological phenomena. To avoid this possibility, a computer algorithm searches out and rejects the major sferic events.

The signal to noise ratio was further improved by the application of a low pass linear digital filter. This filter has zero phase shift which prevents any lag or peak displacement from occurring, and it suppresses only variations with a wavelength less than the specified filter wavelength.

VTEM's X-component data produces crossover type anomalies with conductors located beneath the inflection between maxima and minima in the data. This is in contrast to the Z component which shows maxima or minima above conductors. During acquisition the convention is for X-coil data to be positive in the direction of flight. In the processing phase the polarity is adjusted to follow the right hand rule for multi-component transient electromagnetic methods.

For N-S lines the sign convention for the X in-line component crossover is positive-negative pointing south to north for vertical plate conductors perpendicular to the profile. For E-W lines the sign convention for the X in-line component crossover is positive-negative pointing west to east for vertical plate conductors perpendicular to the profile. X-component data for alternating/opposite flight directions are reversed (multiplied by negative one) in the final database to account for this polarity convention.

The Fraser Filter converts crossovers of the correct polarity into peak responses of X component by differencing successive values. It is calculated as $(f_1+f_2)-(f_3+f_4)$ where f_i are data from four consecutive stations. This is a derivative filter and likely to increase any noise in data.

A useful presentation of X-component data is the Staked Fraser Filter. The Stacked Fraser Filter data are calculated as the average value of 12 channels (25 to 36) of Fraser Filtered X-component data. The signal to noise ratio is improved and information from 12 channels are combined into one, which allows easier presentation in grid or map format.

3.4. Magnetic Data

The processing of the magnetic data involved the correction for diurnal variations by using the digitally recorded ground base station magnetic values. The base station magnetometer data was edited and merged into the Geosoft GDB database on a daily basis. The aeromagnetic data was corrected for diurnal variations by subtracting the observed magnetic base station deviations.

A micro-levelling procedure was then applied. This technique is designed to remove persistent low-amplitude components of flight-line noise remaining after tie line levelling.

The corrected magnetic data was interpolated between survey lines using a random point gridding method to yield x-y grid values for a standard grid cell size of a quarter of the line spacing. The Minimum Curvature algorithm was used to interpolate values onto a rectangular regular spaced grid.

3.5. Digital Terrain Model

Subtracting the radar altimeter data from the GPS elevation data creates a digital elevation model. To correct for minor elevation differences that are evident in this data when gridded, Shuttle Radar Topography Mission (SRTM) data have been used.

4. DELIVERABLES

VTEM Survey and logistics report		
Format	PDF	
Copies	2 x Digital (DVD/CD) 2 x Hard copy	
Database		
Format	Digital Geosoft (.GDB) and ASEG-GDF (.DAT, .DFN and PRJ)	
Channels	Name	Description
	X_UTM	X positional data (UTM Z55S/ WGS84)
	Y_UTM	Y positional data (UTM Z55S/ WGS84)
	X_MGA	X positional data (MGA Z55/ GDA94)
	Y_MGA	Y positional data (MGA Z55/ GDA94)
	Lon	Longitude data
	Lat	Latitude data
	Z	GPS antenna elevation (metres above sea level)
	Radar	Helicopter terrain clearance from radar altimeter (metres above ground level)
	RxAlt	EM Receiver and Transmitter terrain clearance (metres above ground level)
	DTM	Digital terrain model (metres)
	Gtime1	UTC time (seconds of the day)
	MagTF	Raw Total Magnetic field data (nT)
	MagBase	Magnetic diurnal variation data (nT)
	MagDiu	Total Magnetic field diurnal variation and lag corrected data (nT)
	MagMicL	Microleveled Total Magnetic field data (nT)
	dBdtZ[13] to dBdtZ[47]	dB/dt, Time Gates 83 µs to 9286 µs (pV/A/m^4)
	BfieldZ[13] to BfieldZ[47]	B-field, Time Gates 83 µs to 9286 µs (pV.ms/A/m^4)
	dBdtX[20] to dBdtX[47]	dBdtX, Time Gates 220 µs to 9286 µs (pV/A/m^4)
	BfieldX[20] to BfieldX[47]	B-fieldX, Time Gates 220 µs to 9286 µs (pV.ms/A/m^4)
	dBdtX_Pol[20] to dBdtX_Pol[47]	Polarity corrected dB/dtX, Time Gates 220 µs to 9286 µs (pV/A/m^4)
	BfieldX_Pol[20] to BfieldX_Pol[47]	Polarity corrected B-fieldX, Time Gates 220 µs to 9286 µs (pV.ms/A/m^4)
	dBdtX_FF[20] to dBdtX_FF[47]	Fraser Filter dB/dtX, Time Gates 220 µs to 9286 µs (pV/A/m^4)
	BfieldX_FF[20] to BfieldX_FF[47]	Fraser Filtered B-fieldX, Time Gates 220 µs to 9286 µs (pV.ms/A/m^4)
	dBdtX_SFF	Stacked Fraser Filtered data from channel 20 to 36 (pV/A/m^4)
	BfieldX_SFF	Stacked Fraser Filtered data from channel 20 to 36 (pV.ms/A/m^4)
	PLM	Power line monitor

Grids		
Format	Digital Geosoft (.GRD and .GI)[1] and ER Mapper (.ERS)	
Grids	Name	Description
	AA1053_***blk***[2]_Mag	Total Magnetic field (nT)

Maps		
Format	Digital Geosoft (.MAP)	
Scale	1:10 000	
Maps	Name	Description
	AA1053_***blk***_Mag	Total Magnetic field colour contours
	AA1053_***blk***_dBdt_Log	VTEM dB/dt profiles, Time Gates 0.667 – 9.286 ms in log-linear scale
	AA1053_***blk***_Bfield_Log	VTEM B-field profiles, Time Gates 0.667 – 9.286 ms in log-linear scale
	AA1053_***blk***_dBdt_SFF	dBdt X Stacked Fraser Filter (channel 20 - 36)
	AA1053_***blk***_Bfield_SFF	Bfield X Stacked Fraser Filter (channel 20 - 36)

Waveform		
Format	Digital Excel Spreadsheet (AA1053_VTEM_Waveform.xls)	
Columns	Name	Description
	Time	Sampling rate interval, 5.208 µs
	Volt	Output voltage of the receiver coil (volt)
	Current	Transmitter current (normalised to 1A peak)

Google Earth Flight Path file	
Format	Google Earth AA1053_FlightPath.kmz
	Free version of Google Earth software can be downloaded from, *http://earth.google.com/download-earth.html*

---

[1] A Geosoft .GRD file has a .GI metadata file associated with it, containing grid projection information.
[2] _***blk*** indicates the block name

5. PERSONNEL

Geotech Airborne Limited Personnel	
Operator / Crew chief	Jon Lambert
Operator	Peter Hamilton
Technical Support	Tom Eling
Data Processing (Preliminary)	Peter Holbrook
Data Processing (Final) /Reporting	Evans Bauren
Final data supervision	Malcolm Moreton Data Processing Manager (malcolm@geotechairborne.com)
Overall project management	Keith Fisk Managing Partner and Director (keith@geotechairborne.com)

APPENDIX A

GENERALIZED MODELING RESULTS OF THE VTEM SYSTEM

(by Roger Barlow and Alexander Prikhodko)

Introduction

The VTEM system is based on a concentric or central loop design, whereby, the receiver is positioned at the centre of a transmitter loop that produces a primary field. The wave form is a bi-polar, modified square wave with a turn-on and turn-off at each end.

During turn-on and turn-off, a time varying field is produced (dB/dt) and an electro-motive force (emf) is created as a finite impulse response. A current ring around the transmitter loop moves outward and downward as time progresses. When conductive rocks and mineralization are encountered, a secondary field is created by mutual induction and measured by the receiver at the centre of the transmitter loop.

Efficient modeling of the results can be carried out on regularly shaped geometries, thus yielding close approximations to the parameters of the measured targets. The following is a description of a series of common models made for the purpose of promoting a general understanding of the measured results.

A set of models has been produced for the Geotech VTEM® system dB/dT Z and X components (see models A-1 to A-16). The Maxwell ™ modeling program (EMIT Technology Pty. Ltd. Midland, WA, AU) used to generate the following responses assumes a resistive half-space. The reader is encouraged to review these models, so as to get a general understanding of the responses as they apply to survey results. While these models do not begin to cover all possibilities, they give a general perspective on the simple and most commonly encountered anomalies.

As the plate dips and departs from the vertical position, the peaks become asymmetrical.

As the dip increases, the aspect ratio (Min/Max) decreases and this aspect ratio can be used as an empirical guide to dip angles from near 90º to about 30º. The method is not sensitive enough where dips are less than about 30º.

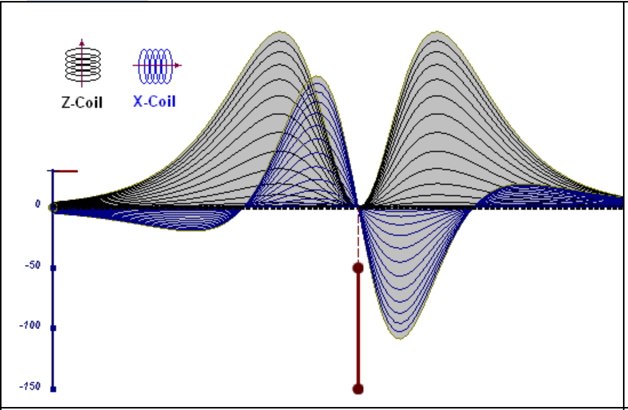

Fig A-1: Vertical thin plate

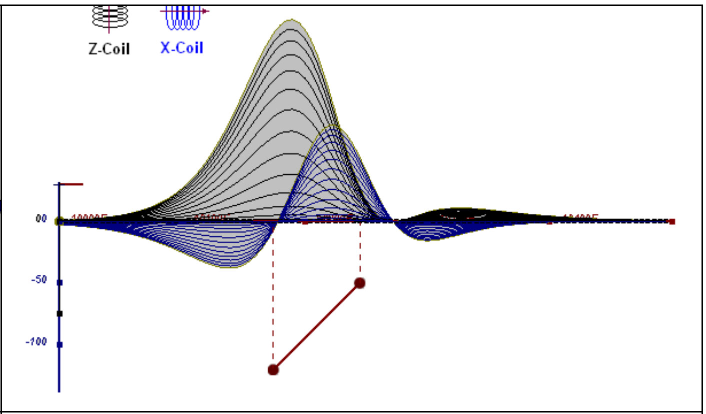

Fig A-2: Inclined thin plate

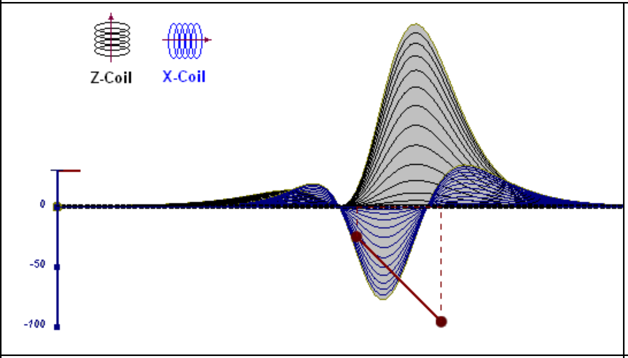

Fig A-3: Inclined thin plate

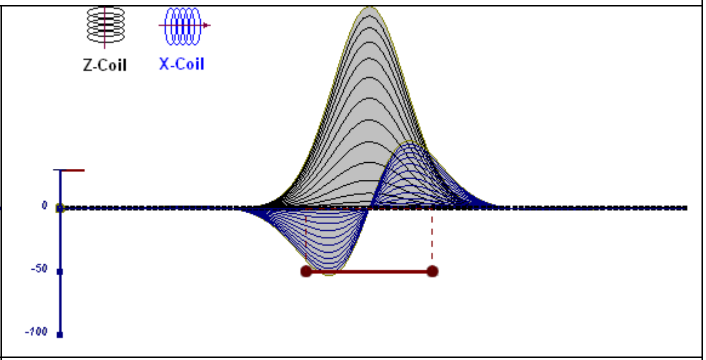

Fig A-4: Horizontal thin plate

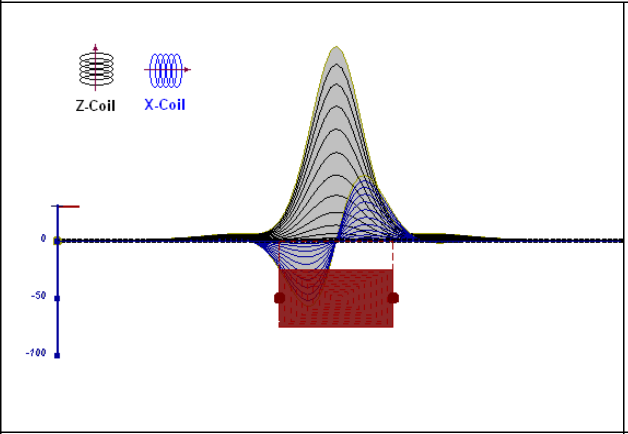

Figure A-5: Horizontal thick plate (linear scale of the response)

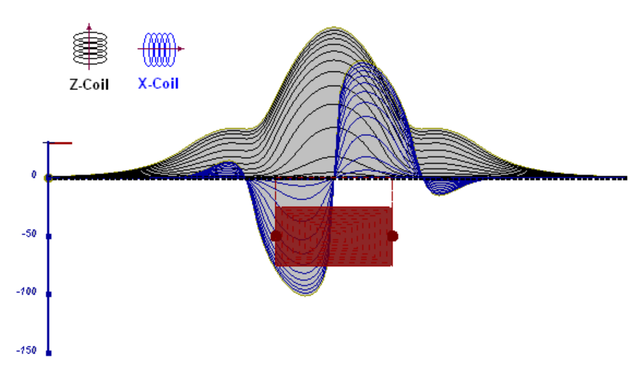

Figure A-6: Horizontal thick plate (log scale of the response)

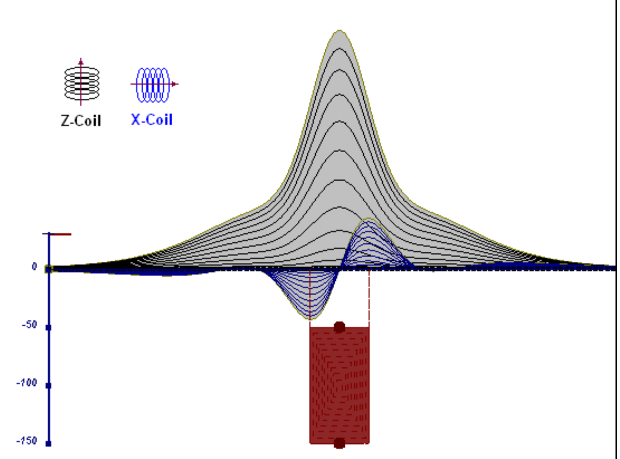

Figure A-7: Vertical thick plate (linear scale of the response). 50 m depth

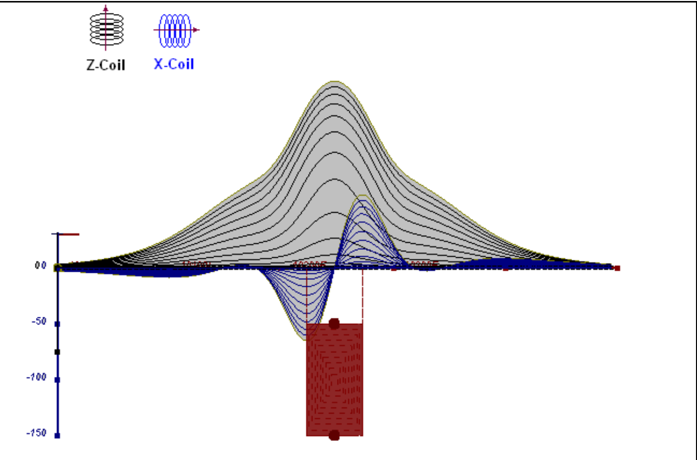

Figure A-8: Vertical thick plate (log scale of the response). 50 m depth

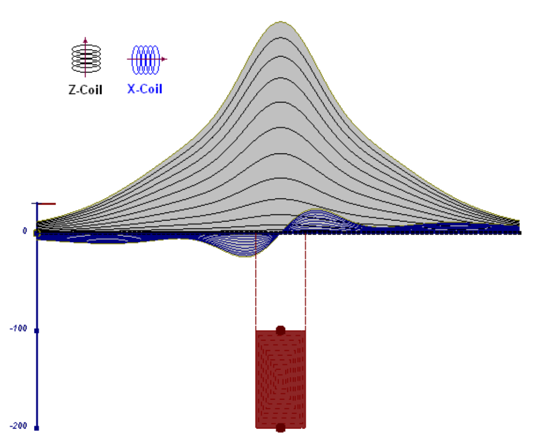

Fig A-9: Vertical thick plate (linear scale of the response). 100 m depth

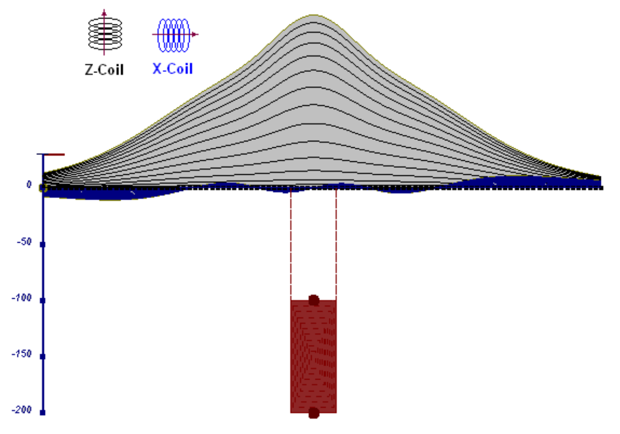

Fig A-10: Vertical thick plate (linear scale of the response). Depth/hor.thickness=2.5

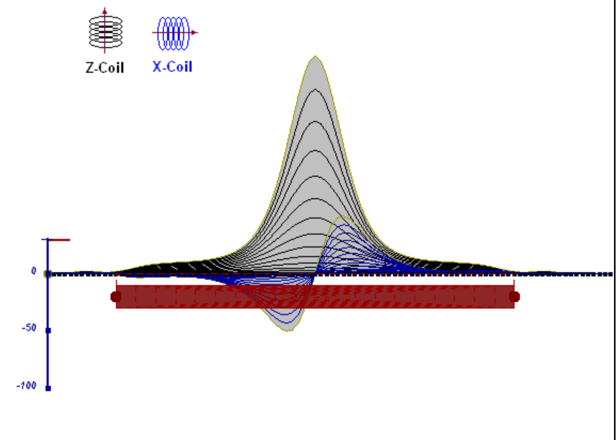

Fig A-10: Horizontal thick plate (linear scale of the response)

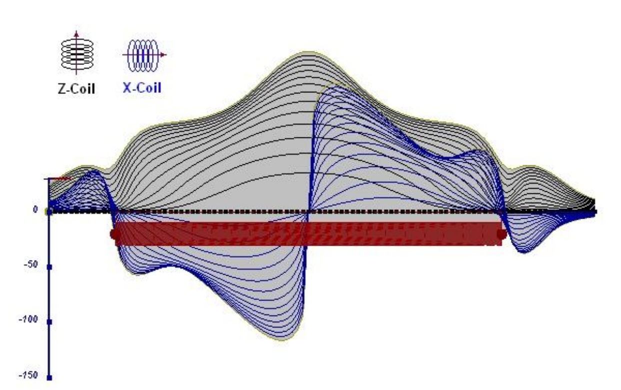

Fig A-11: Horizontal thick plate (log scale of the response)

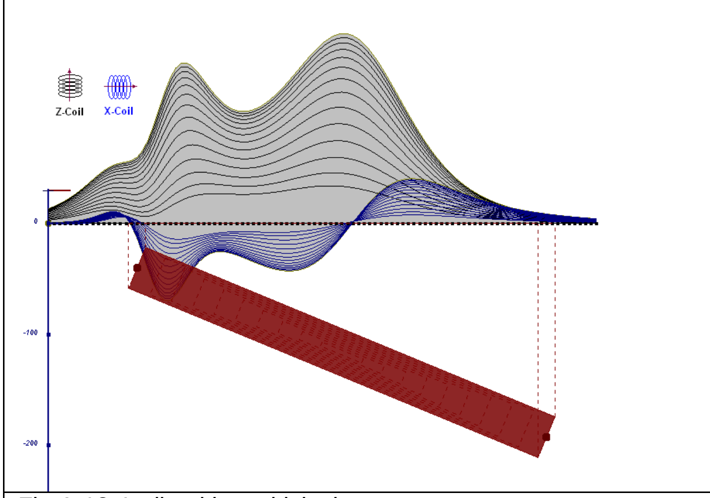

Fig A-12: Inclined long thick plate

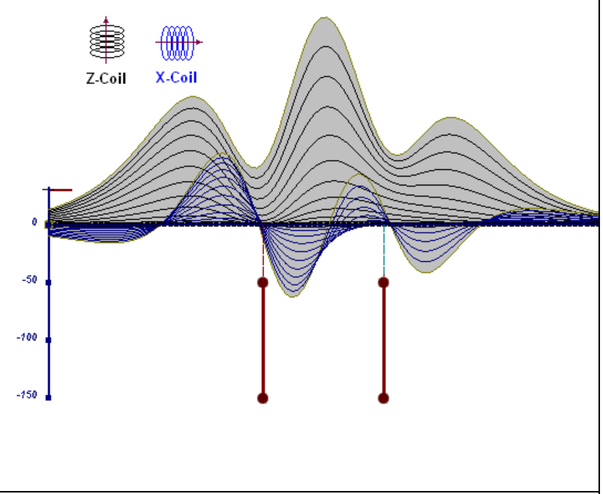

Fig A-13: Two vertical thin plates

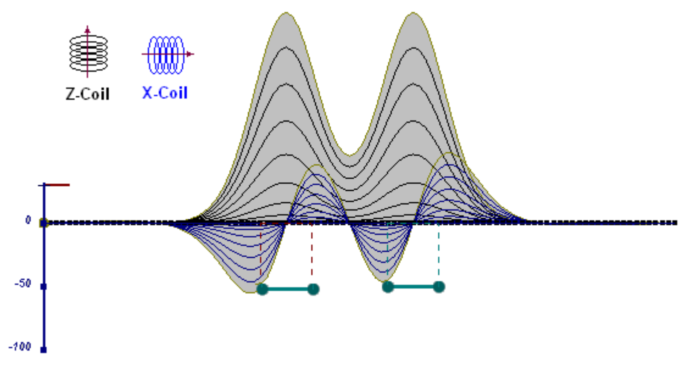

Fig A-14: Two horizontal thin plates

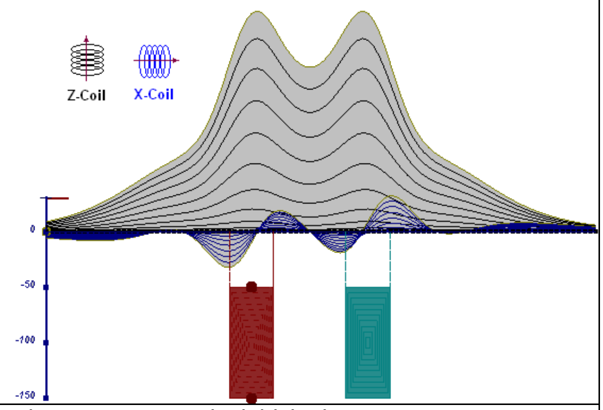

Fig A-15: Two vertical thick plates

The same type of target but with different thickness, for example, creates different form of the response:

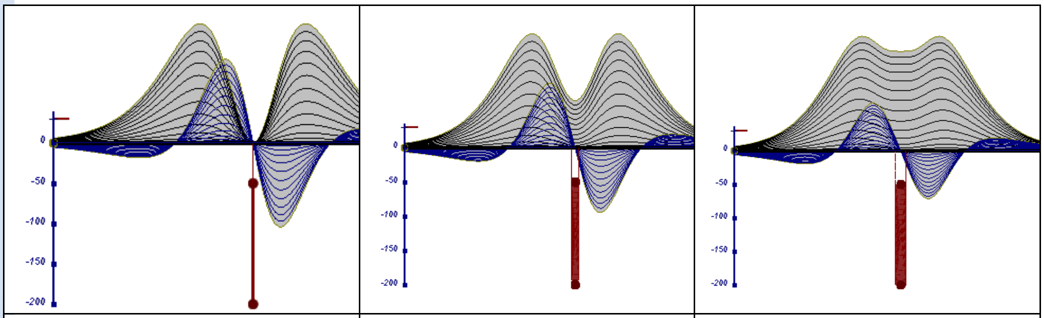

“thin” | 10 m thickness | 15 m thickness

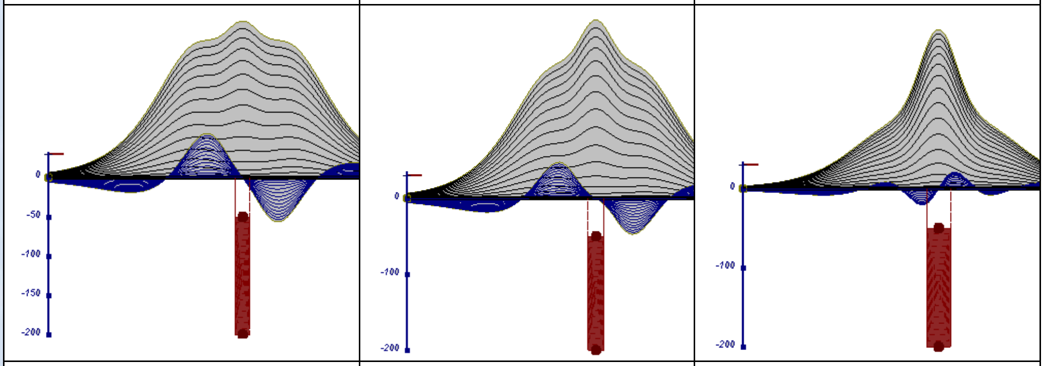

18 m thickness | 20 m thickness | 30 m thickness

Fig A-16 Conductive vertical plate, depth 50 m, strike length 200 m, depth extend 150 m.

General Interpretation Principals

Magnetics

The total magnetic intensity responses reflect major changes in the magnetite and/or other magnetic minerals content in the underlying rocks and unconsolidated overburden. Precambrian rocks have often been subjected to intense heat and pressure during structural and metamorphic events in their history. Original signatures imprinted on these rocks at the time of formation have, it most cases, been modified, resulting in low magnetic susceptibility values.

The amplitude of magnetic anomalies, relative to the regional background, helps to assist in identifying specific magnetic and non-magnetic rock units (and conductors) related to, for example, mafic flows, mafic to ultramafic intrusives, felsic intrusives, felsic volcanics and/or sediments etc. Obviously, several geological sources can produce the same magnetic response. These ambiguities can be reduced considerably if basic geological information on the area is available to the geophysical interpreter.

In addition to simple amplitude variations, the shape of the response expressed in the wave length and the symmetry or asymmetry, is used to estimate the depth, geometric parameters and magnetization of the anomaly. For example, long narrow magnetic linears usually reflect mafic flows or intrusive dyke features. Large areas with complex magnetic patterns may be produced by intrusive bodies with significant magnetization, flat lying magnetic sills or sedimentary iron formation. Local isolated circular magnetic patterns often represent plug-like igneous intrusives such as kimberlites, pegmatites or volcanic vent areas.

Because the total magnetic intensity (TMI) responses may represent two or more closely spaced bodies within a response, the second derivative of the TMI response may be helpful for distinguishing these complexities. The second derivative is most useful in mapping near surface linears and other subtle magnetic structures that are partially masked by nearby higher amplitude magnetic features. The broad zones of higher magnetic amplitude, however, are severely attenuated in the vertical derivative results. These higher amplitude zones reflect rock units having strong magnetic susceptibility signatures. For this reason, both the TMI and the second derivative maps should be evaluated together.

Theoretically, the second derivative, zero contour or colour delineates the contacts or limits of large sources with near vertical dip and shallow depth to the top. The vertical gradient map also aids in determining contact zones between rocks with a susceptibility contrast, however, different, more complicated rules of thumb apply.

Concentric Loop EM Systems

Concentric systems with horizontal transmitter and receiver antennae produce much larger responses for flat lying conductors as contrasted with vertical plate-like conductors. The amount of current developing on the flat upper surface of targets having a substantial area in this dimension, are the direct result of the effective coupling angle, between the primary magnetic field and the flat surface area. One therefore, must not compare the amplitude/conductance of responses generated from flat lying bodies with those derived from near vertical plates; their ratios will be quite different for similar conductances.

Determining dip angle is very accurate for plates with dip angles greater than 30º. For angles less than 30º to 0º, the sensitivity is low and dips cannot be distinguished accurately in the presence of normal survey noise levels.

A plate like body that has near vertical position will display a two shoulder, classic **M** shaped response with a distinctive separation distance between peaks for a given depth to top.

It is sometimes difficult to distinguish between responses associated with the edge effects of flat lying conductors and poorly conductive bedrock conductors. Poorly conductive bedrock conductors having low dip angles will also exhibit responses that may be interpreted as surfacial overburden conductors. In some situations, the conductive response has line to line continuity and some magnetic correlation providing possible evidence that the response is related to an actual bedrock source.

The EM interpretation process used, places considerable emphasis on determining an understanding of the general conductive patterns in the area of interest. Each area has different characteristics and these can effectively guide the detailed process used.

The first stage is to determine which time gates are most descriptive of the overall conductance patterns. Maps of the time gates that represent the range of responses can be very informative. Next, stacking the relevant channels as profiles on the flight path together with the second vertical derivative of the TMI is very helpful in revealing correlations between the EM and Magnetics. Key lines can be profiled as single lines to emphasize specific characteristics of a conductor or the relationship of one conductor to another on the same line.

Resistivity Depth sections can be constructed to show the relationship of conductive overburden or conductive bedrock with the conductive anomaly.

APPENDIX B

GEOPHYSICAL MAP IMAGES
(not to scale)